Benha Journal of Applied Sciences (BJAS) *print: ISSN 2356–9751*
Vol. (1) (2016),107-116 *online: ISSN 2356–976x*
http:// bjas.bu.edu.eg

Net Charge Fluctuations and Chemical Freez-out Conditions

A.Tawfik [1, 2], L.I.Abou-Salem [2], Asmaa Shalaby [2, 3], M.Hanafy [2]
1 Egyptian Center for Theoretical Physics (ECTP), Modern University for Technology and Information (MTI), 11571 Cairo, Egypt
2World Laboratory for Cosmology and Particle Physics (WLCAPP), Cairo, Egypt
3 Physics Department, Faculty of Science, Benha University, 13518, Benha, Egypt.
E- mail: atawfik@cern.ch

Abstract

Different freeze-out conditions such as energy per particle density, baryon and anti-baryon density, normalized entropy density and constant trace anomaly are analyzed. These cretiteria for chemical freeze-out are calculated in framework of the hadron resonance gas (HRG) model. A systematic comparison with recent experimental data is presented. The Dependence of particle ratios on beam energy is extracted. The net charge fluctuations ν_{dyn} for different species K/π, P/π, and K/P are studied and compared with STAR measurements from Au+Au collisions at $\sqrt{S_{NN}}$=7.7-200 GeV. We find a satisfied agreement with the experimental results and furthermore conclude that the HRG model is suitable to explain the dynamical net charge fluctuations.

1. Introduction

Hadronic matter is studied in heavy-ion experiments under extreme conditions of high temperature, density or both of them [1]. In a few microseconds from Big Bang, the new state of matter, quark-gluon plasma (QGP), should be created [2]. On other hand, quantum chromodynamics (QCD) predicts that strongly interacting matter undergoes a phase transition from the hadronic state to a system of deconfined quarks and gluons; QGP [3]. The particle yields is considered one of the most important results obtained from relativistic heavy-ion collisions at different beam energies and can be described by thermal-statistical models [4-18]. It is supposed that, the chemical equilibrium has only two parameters; the temperature (T) and baryon chemical potential μ_b [19-27]. After hadronization, the particles interact strongly with each others at distances is of order 1 fm, and later on the system would reach a state of chemical equilibrium refering to the composition of the fireball [28]. Hence, the chemical equilibrium means that the rate of creation and annihilation will be exactlly equal. This evolution process continues until the hadron gas cools down, i.e. chemical freeze-out. The chemical freez-out is the point at which the inelastic collisions cease and all particle ratios are frozen.

A second form of particle equilibrium is the thermal freeze-out, where the produced particles (their number is fixed in stage of chemical freeze-out) continue interacting, elastically. The fireball continues expanding and cooling until these interactions cease. By observing the particle abundances which reflec the properties of the system at chemical freez-out, one finds that at Super Proton Synchrotron SPS energies the particle distribution becomes characterstic at T=170 MeV [29]. By observing the particle momentum distributions which characterize the system at thermal freez-out, one can conclude that the thermal freez-out occurs later at T=130 MeV at same SPS energies.

The hadron Resonance Gas (HRG) model seems to give a good description for the thermal evolution of the thermodynamic quantities in the hadronic matter [7-10] and has been successfully utilized to characterize the conditions deriving the chemical freez-out [28-31]. Also the partition function used in heavy-ion collisions has shown an agreement with the results obtained from lattice QCD in the hadronic phase [30]. It is found with increasing the collision energy, the chemical freeze-out temperature, T, increases while the corresponding baryon chemical potential, μ_b, decreases. In lattice QCD [31-32], the phase diagram is studied from low energy Schwerionensynchrotron SIS to high energy, Relativistic Heavy Ion Collider, RHIC with a critical temperature T=170 MeV at vanishingchemical baryon potential. The study of the freez-out conditions is essential in extracting the particle spectra and particle excitation function, since we can know the number of resonances, their widths, and the treatment of weak decays [19].

Different freze-out conditions are studied,

e.g. $\frac{E}{N} \approx 1GeV$ [33-34] and a baryon and anti-baryon densities, $n_B + n_{\bar{B}} \approx 0.12\ fm^{-3}$ [29], normalized entropy, $s/T^3=7$ and the trace anomaly $(\varepsilon - 3p)/T_4 = 7/2$ [2,35-38]. We compare the HRG calculations with data from SIS [33-34,40], Alternating Gradient Synchrotron AGS, SPS [39-41] and RHIC [42-47].

The present paper is organized as follows; section II is devoted to study the HRG model, the thermodynamical quantities, e.g. number density and pressure are derived using the grant canonical partition function. The parameterization of the baryonic chemical potential on the dependence of $\sqrt{S_{NN}}$ is showed. In Section III, the net charge fluctuations as a signal of QGP are calculated. The particle ratios are studied at different energies. In Section IV, the results from different freeze-out conditions, particle ratios and net charge fluctuations for K/π, P/π, and K/P are presented. In Section V, summary and conclusion are outlined.

2. Formalism

The thermodynamics can be extracted simply from the partition function $Z(T,V)$. The grand canonical partition function [29] is given by

$$Z^{GC}(T,V,\mu_Q) = Tr[EXP - \beta(H - \sum_i \mu_Q Q_i)] \quad (1)$$

where H is the Hamiltonian of the system, Q_i are the conserved charges and μ_Q are the chemical potentials and $\beta = \frac{1}{T}$. The Hamiltonian is used in the partition function because it contains all relevant degrees off freedom of the confiend and the strongly interacting medium implicity includes other types of interactions that results in resonances formation.

Therefore the partition function (1) of a hadron resonance gas can be written as [29]

$$\ln Z(T,V,\overrightarrow{\mu}) = \sum_i lnZ_i(T,V,\overrightarrow{\mu}) \quad (2)$$

where $\overrightarrow{\mu} = (\mu_B, \mu_S, \mu_Q)$ are the chemical potentials related to baryon number, strangness and electric charge, respictively.

$$lnZ_i\left(T,V,\overrightarrow{\mu}\right) = \frac{Vg_i}{2\pi^2}\int_0^\infty \pm p^2\, dp \ln[1 \pm \lambda_i \exp(-\beta\varepsilon_i)] \quad (3)$$

where +ive and -ive sign stand for bosons and fermions, respectively, $\varepsilon_i = \sqrt{p^2 + m_i^2}$ and the fugacity factor λ_i [29] is given by

$$\lambda_i(T,\vec{\mu}) = exp(\frac{B_i\mu_B + S_i\mu_S + Q_i\mu_Q}{T}) \quad (4)$$

Expressing the partition function (3) in terms of Bessel function [29], one ge

$$lnZ_i(T,V,\overrightarrow{\mu}) = \frac{VTg_i}{2\pi^2}\sum_{k=1}^{\infty}\frac{\pm^{k+1}}{k^2}\lambda_i^k m_i^2 K_2(\frac{km_i}{T}) \quad (5)$$

where K_2 is the second order modified Bessel function.

The number density of particles per unit volume is obtained from (5) as the following [29]

$$n_i(T,\overrightarrow{\mu}) = \frac{\langle N_i \rangle}{V} = \frac{Tg_i}{2\pi^2}\sum_{k=1}^{\infty}\frac{\pm^{k+1}}{k^2}\lambda_i^k m_i^2 K_2(\frac{km_i}{T}) \quad (6)$$

At finite temperature T and baryon chemical potential μ_i, the pressure of the i-th hadron or resonance is given as [29]

$$p(T,\mu_i) = \pm\frac{g_i}{2pi^2}T\int_0^\infty k^2 dk \ln(1 \pm [(\mu_i - \varepsilon_i)/T]) \quad (7)$$

In order to calculate all particle ratio, the parametes we need are the chemical potentials, temperature, degenercy factor and volume. We will calculte the chemical potential and temperature from Tawfik [1-2,7-10] realtion that related them to the energy as the following

$$\mu_B = \frac{a}{1 + b\sqrt{S_{NN}}} \quad (8)$$

where $\sqrt{S_{NN}}$ is in GeV, a=1.245±0.094 GeV and b=0.264±0.028 GeV^{-1}. Also the dependence of the chemical freeze-out temperature T_{ch} on $\sqrt{S_{NN}}$ can be parametrized as [34]

$$T_{ch} = T_{lim}(\frac{1}{1 + exp[\frac{1.172 - ln(\sqrt{S_{NN}})}{0.45}]}) \quad (9)$$

where the limiting temperature is, $T_{lim} = 164MeV$.

Another relation suggested by Cleymans [34] shows that the baryonic potential can be fitted to the beam energy using the following formula

$$\mu_B(s) \approx \frac{a}{1+\frac{\sqrt{s}}{b}} \quad (10)$$

3. Net Charge Fluctuation

Phase transition has well known signatures such as fluctuations of the net charge. A significant fluctuation occurs when the QGP undergoes phase transition to the hadronic one [46-47]. The Relativistic Heavy Ion Collider (RHIC) start to search for the QCD critical point by making an energy scan of Au+Au collisions from low collision energy ($\sqrt{S_{NN}}$=7.7 GeV) up to high energies ($\sqrt{S_{NN}}$=200 GeV). The net charge fluctuations as a signal of quark-gloun plasma (QGP) are calculated in terms of the parameter ν_{dyn}.

The definition of $\nu_{dyn,k/\pi}$ which describes fluctuations in K/π ratio is given by [46]

$$\nu_{dyn,k/\pi} = \frac{<N_K(N_K-1)>}{<N_K>^2} + \frac{<N_\pi(N_\pi-1)>}{<N_\pi>^2} - 2\frac{<N_K N_\pi>}{<N_K><N_\pi>} \quad (11)$$

We calculated the charge dependence of the dynamical K/π, P/π, and K/P fluctuations and make comparison with STAR experiment results. The charge dependence of the dynamical K/π, P/π, and K/P fluctuations are calculated and compared with STAR results [46].

Similarly, formula for P/π, and K/P ratios can be constructed as in Eq.(11). For more details readers are advised to consult Refs. [49-50].

4 -Results and Discussion

The dependence of freeze-out temperature T on the baryon chemical potential μ_b at different freeze-out conditions is given in Fig. 1. In Fig. 1a, he temperature is plotted versus μ_b at fixed E/N≈1.02 GeV.

Fig. (1b) shows the (T-μ_b) dependence in case of , $s/T^3=7$ where s is the entropy. Fig. (1c) shows the (T-μ_b) dependence using the following condition ;$n_B + n_{\bar{B}} = 0.12\ \text{fm} - 3$; where $n_B and\ n_{\bar{B}}$ are the sum of baryon and anti-baryon densities respictively. Finally, fig. (1d) shows the (T-μ_b) dependence in case of using the QCD trace anomaly condition which is defined as $(\varepsilon - 3p)/T_4 = 7/2$. From figs.(1), one can notice that; at vanishing chemical potential, the freeze-out temperature T_f is taking the values ; $164 \le T_f \le 169$ MeV; and this value is close to that of undergoes phase transition as known from lattice gauge theory that give an upper limit of about 170 MeV [29,51]. Also there is a great discrepancy at higher μ_b values ($\mu_b \ge 650$ MeV).

In Figs.(2a-2i), the calculated charge dependence of the dynamical K/π, P/π, and K/P fluctuations compared to with STAR experiment results.

Fig.(2a) , (2b), and (2c) shows $\nu_{dyn,k/\pi}$ as a function of the energy compared to STAR data measured in central 0-5% Au+Au collisions at $\sqrt{S_{NN}}$=7.7-200 GeV. The total dynamical fluctuation $\frac{K}{\pi}$ are setted as $\frac{K}{\pi} = \frac{K^+ + K^-}{\pi^+ + \pi^-}$ as shown in fig.(2a) where the volume of the fire ball is taken as 770.72 ± 77 fm^3. Only the $\nu_{dyn,k/\pi}$ in case of $\frac{K}{\pi} = \frac{K^+ + K^-}{\pi^+ + \pi^-}$ have positive values. In fig.(2b),

The total dynamical fluctuation $\frac{K}{\pi}$ are setted as $\frac{K}{\pi} = \frac{K^+}{\pi^+} + \frac{K^-}{\pi^-}$,where we take the average of the same sign and the volume of the fire ball is taken as 1.43 ± 0.143 fm^3. In fig.(2c), the average of the opposite sign is considered where $\frac{K}{\pi} = \frac{K^+}{\pi^-} + \frac{K^-}{\pi^+}$ and the volume of the fire ball is taken as; 1.82 ± 0.182 fm^3. One can see that we have a satisfied agreement with the experimental data in case of the different $\frac{K}{\pi}$ dynamical fluctuations.

Fig.(2d), (2e), and (2f) shows $\nu_{dyn,P/\pi}$ as a function of the energy in comparison with STAR experiment measured in central 0-5% Au+Au collisions at $\sqrt{S_{NN}}$=7.7-200 GeV. The total dynamical fluctuation $\frac{P}{\pi}$ are setted as $\frac{P}{\pi} = \frac{P^+ + P^-}{\pi^+ + \pi^-}$ as shown in fig.(2d) where the volume of the fire ball is taken as 2.052 ± 0.2052 fm^3. In fig.(2e), the total dynamical fluctuation $\frac{P}{\pi}$ are setted as $\frac{P}{\pi} = \frac{P^+}{\pi^+} + \frac{P^-}{\pi^-}$,where we take the average of the same sign and the volume of the fire ball is taken as 1.56 ± 0.156 fm^3. In fig.(2f), the average of the opposite sign is considered where $\frac{P}{\pi} = \frac{P^+}{\pi^-} + \frac{P^-}{\pi^+}$ and the volume of the fire ball is taken as 1.69 ± 0.169 fm^3. One can see that we have a satisfied agreement with the experimental data in case of the different $\frac{P}{\pi}$ dynamical fluctuations.

Fig.(2g), (2h), and (2i) shows $\nu_{dyn,k/P}$ as a function of the energy in comparison with STAR experiment measured in central 0-5% Au+Au collisions at $\sqrt{S_{NN}}$=7.7-200 GeV. The total dynamical fluctuation $\frac{K}{P}$ are setted as $\frac{K}{P} = \frac{K^+ + K^-}{P^+ + P^-}$ as shown in fig.(2g) where the volume of the fire ball is taken as 2.1 ± 0.21 fm^3. In fig.(2h), The total dynamical fluctuation $\frac{K}{P}$ are written as $\frac{K}{P} = \frac{K^+}{P^+} + \frac{K^-}{P^-}$,where we take the

average of the same sign and the volume of the fire ball is taken as 1.3 ± 0.13 fm^3. In fig.(2i), the average of the opposite sign is considered where $\frac{K}{P} = \frac{K^+}{P^-} + \frac{K^-}{P^+}$ and the volume of the fire ball is taken as 1.3 ± 0.13 fm^3. One can see that we have a satisfied agreement with the experimental data in case of the different $\frac{K}{P}$ dynamical fluctuations..

In figs.(3a-3f), we have shown the energy dependence of the particle ratios $\frac{\pi^-}{\pi^+}$, $\frac{K^-}{K^+}$, $\frac{K^-}{\pi^-}$, $\frac{P^-}{P}$, $\frac{\Lambda^-}{\Lambda}$, and $\frac{\Omega}{\pi^-}$ x 10 respictively in comparison with the avaliable experimental results [38].

From these figures, one can see that $\frac{\pi^-}{\pi^+}$ ratio decreases with increasing the collision energy while $\frac{K^-}{K^+}$, $\frac{K^-}{\pi^-}$, $\frac{P^-}{P}$, and $\frac{\Lambda^-}{\Lambda}$ ratios increases with increasing the collision energy. In case of $\frac{\Omega}{\pi^-}$ ratio (where, in this case the values are multiplied with scale factor 10), one can notice that, this ratio increases with the collision energy untill sharp peak (at $\sqrt{S_{NN}}$ = 25 GeV) and then began to decrease. This behaviour is call as the horn.

In fig.(3g), (3h), and (3i), we have calculated $\frac{\pi^-}{\pi^+}$, $\frac{k^-}{k^+}$, $\frac{\bar{p}}{p}$, $\frac{\bar{\lambda}}{\lambda}$, $\frac{\bar{\Xi}}{\Xi}$ $\frac{k^-}{\pi^-}$, $\frac{k^+}{\pi^+}$, $\frac{\bar{p}}{\pi^-}$, $\frac{p}{\pi^+}$, $\frac{\lambda}{\pi^-}$, $\frac{\bar{\Xi}}{\pi^-}$, and $\frac{\Omega}{\pi^-}$ ratios at STAR beam energies 62, 130, and 200 GeV. One can see a satisfied agreement with the experimental data in case of the all considered particle ratios.

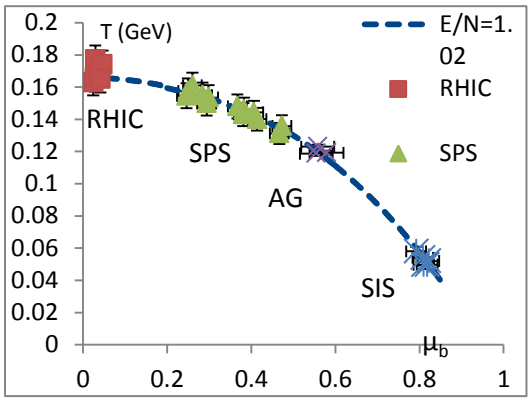

Fig 1a. (T-μ_b) relation at fixed E/N=1.02 GeV compared with data from SIS(lowenergy) to RHIC(High energy) [48].

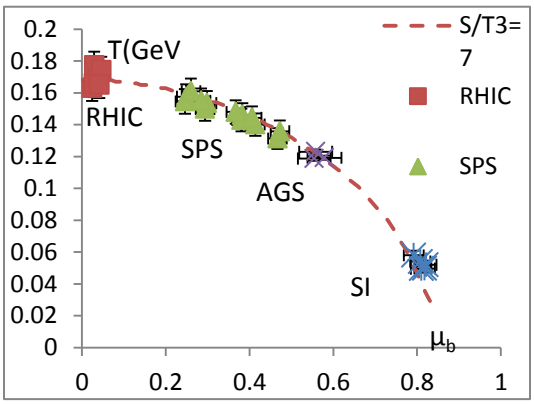

Fig 1b. (T-μ_b) relation at fixed entropy density over T^3 compared with data from SIS(lowenergy) to RHIC(High energy)[48].

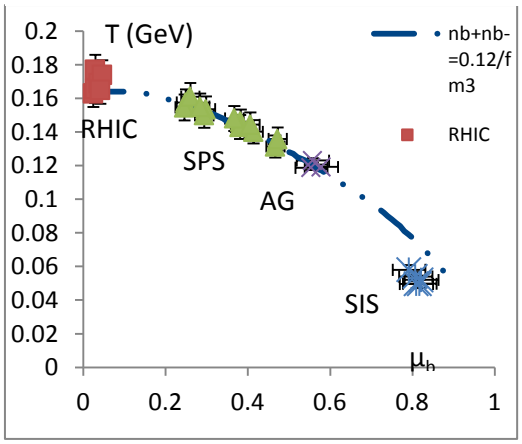

Fig 1c. (T-μ_b) relation at fixed value for the sum of baryon and anti-baryon densities compared with data from SIS(lowenergy) to RHIC(High energy) [48].

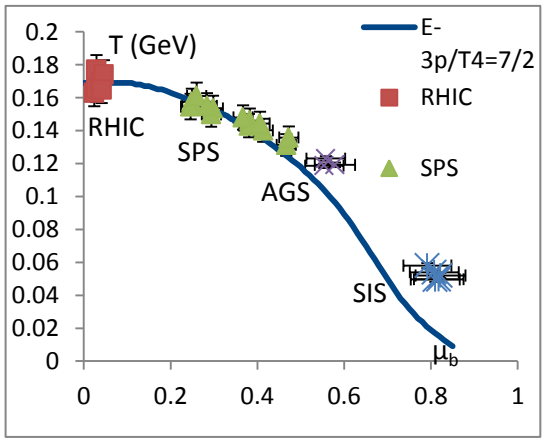

Fig 1d. (T-μ_b) relation at Constant Trace Anomaly as compared with data from SIS(lowenergy) to RHIC(High energy)[48].

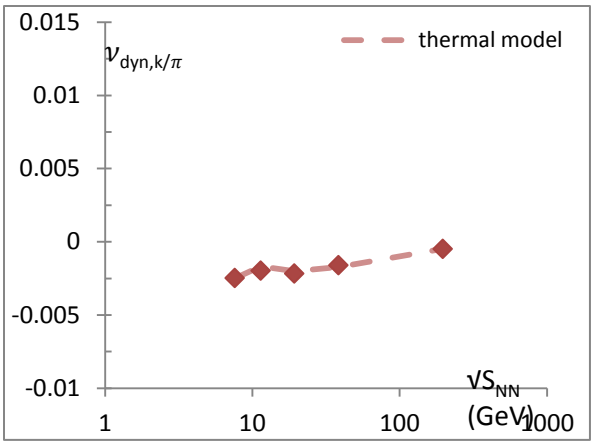

Fig 2a. The calculated $\nu_{dyn,k/\pi}$ $(\frac{K}{\pi} = \frac{K^+ + K^-}{\pi^+ + \pi^-})$ in comparison with STAR experiment [46].

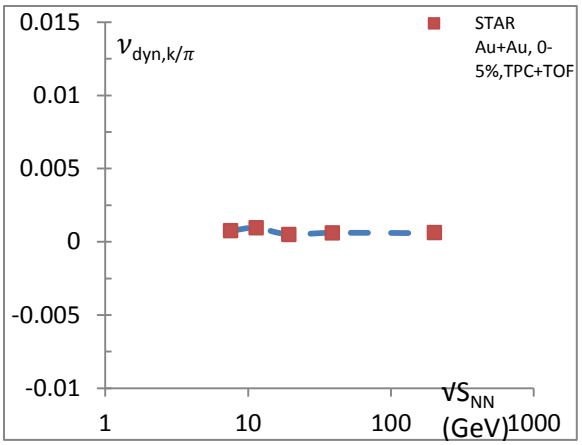

Fig 2b. The calculated $\nu_{dyn,k/\pi}$ for the average of the same sign $(\frac{K}{\pi} = \frac{K^+}{\pi^+} + \frac{K^-}{\pi^-})$ in comparison with STAR experiment [46].

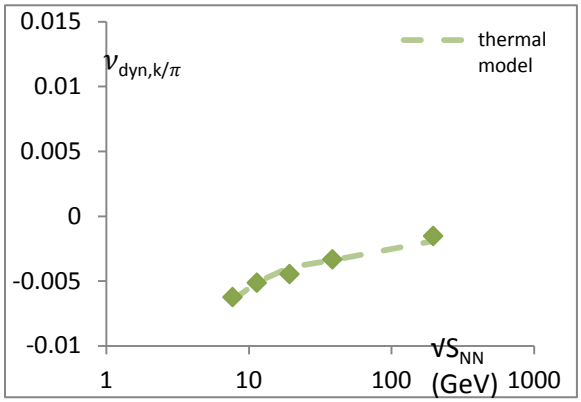

Fig 2c The calculated $\nu_{dyn,k/\pi}$ for the average of the opposite sign $(\frac{K}{\pi} = \frac{K^+}{\pi^-} + \frac{K^-}{\pi^+})$ in comparison with STAR experiment [46].

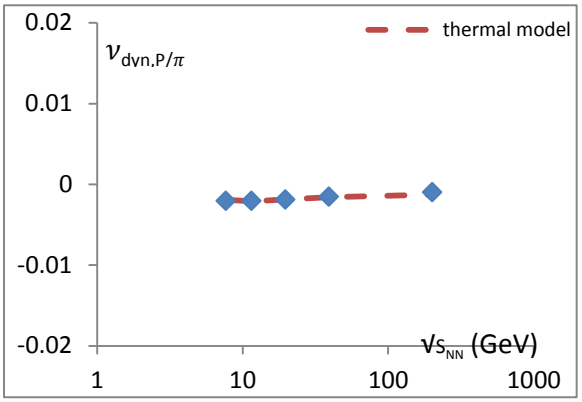

Fig 2d. The calculated $\nu_{dyn,k/\pi}$ $(\frac{P}{\pi} = \frac{P^+ + P^-}{\pi^+ + \pi^-})$ in comparison with STAR experiment [46]

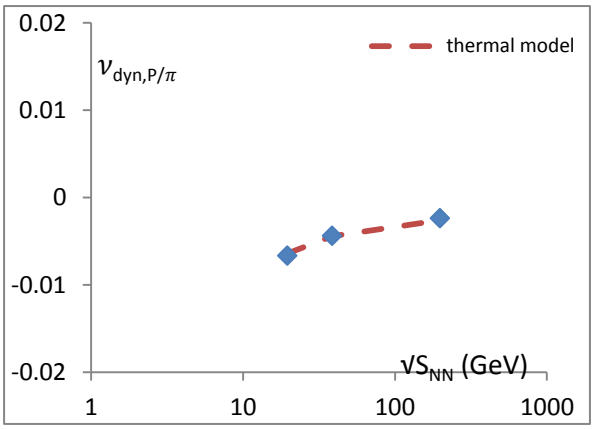

Fig 2e. The calculated $\nu_{dyn,k/\pi}$ for the average of the same sign $(\frac{P}{\pi} = \frac{P^+}{\pi^+} + \frac{P^-}{\pi^-})$ in comparison with STAR experiment [46].

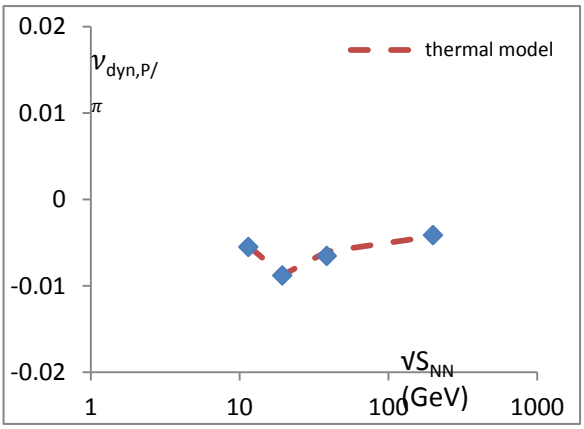

Fig 2f. The calculated $\nu_{dyn,k/\pi}$ for the average of the opposite sign $(\frac{P}{\pi} = \frac{P^+}{\pi^-} + \frac{P^-}{\pi^+})$ in comparison with STAR experiment [46].

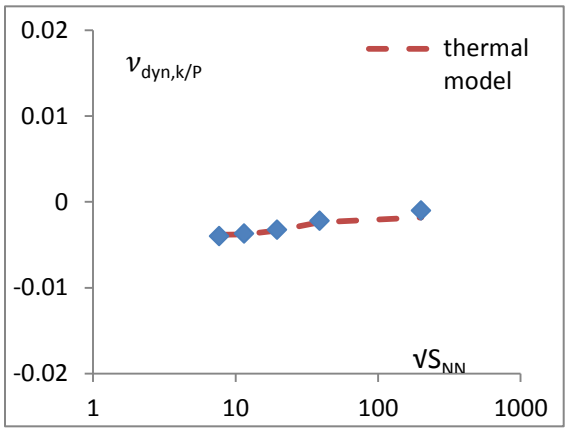

Fig 2g. The calculated $\nu_{dyn,k/\pi}$ ($\frac{k}{P}=\frac{k^{+}+k^{-}}{P^{+}+P^{-}}$) in comparison with STAR experiment [46]

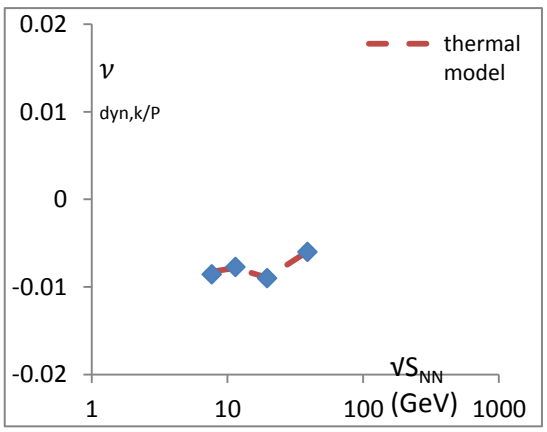

Fig 2h. The calculated $\nu_{dyn,k/\pi}$ for the average of the same sign ($\frac{K}{P}=\frac{K^{+}}{P^{+}}+\frac{K^{-}}{P^{-}}$) in comparison with STAR experiment [46].

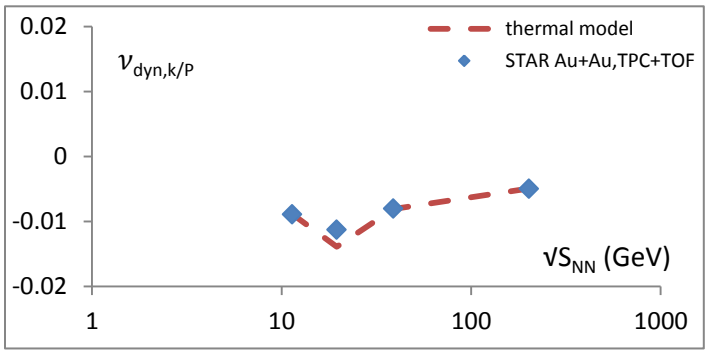

Fig 2i. The calculated $\nu_{dyn,k/\pi}$ for the average of the opposite sign ($\frac{K}{P}=\frac{K^{+}}{P^{-}}+\frac{K^{-}}{P^{+}}$) in comparison with STAR experiment [46].

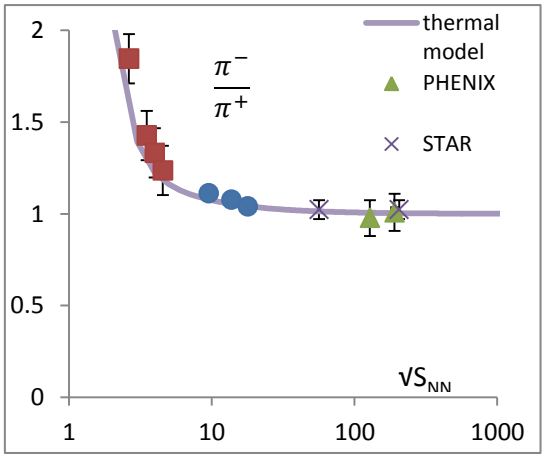

Fig 3a. The energy dependence of particle ratios for $\frac{\pi^{-}}{\pi^{+}}$ in comparison with different experimental results [38].

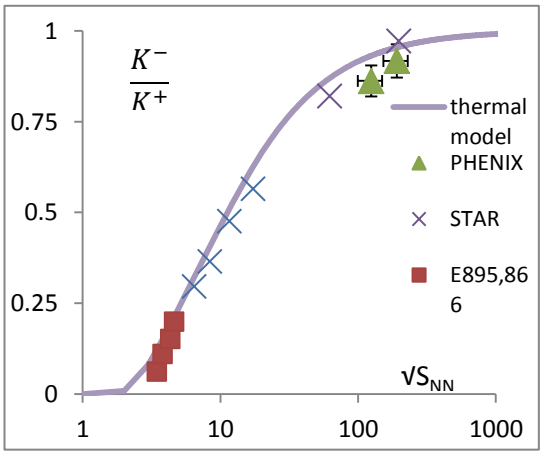

Fig 3b. The energy dependence of particle ratios for $\frac{K^{-}}{K^{+}}$ in comparison with different experimental results [38].

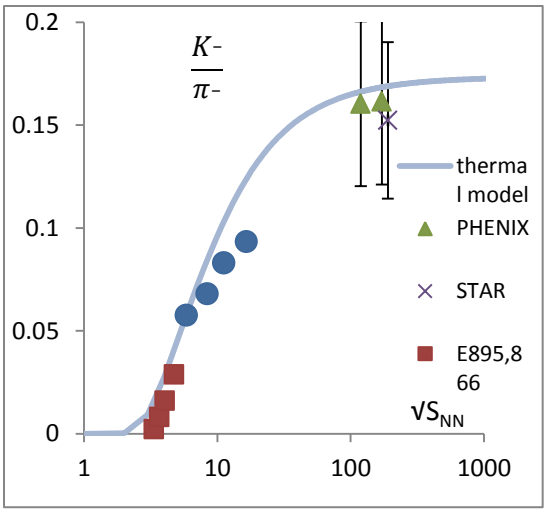

Fig 3c. The energy dependence of particle ratios for $\frac{K^-}{\pi^-}$ in comparison with different experimental results [38].

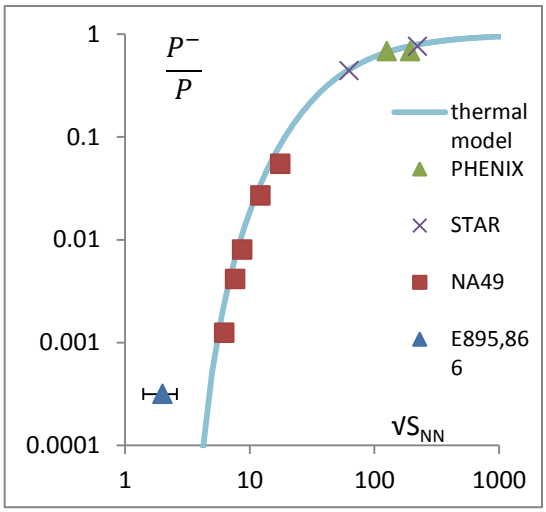

Fig 3d. The energy dependence of particle ratios for $\frac{P^-}{P}$ in comparison with different experimental results [38].

From these figures, one can see that $\frac{\mu}{\pi^+}$ ratio

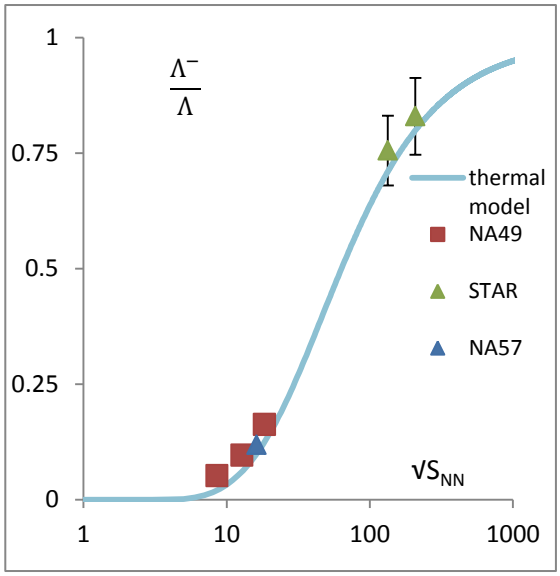

Fig 3e. The energy dependence of particle ratios for $\frac{\Lambda^-}{\Lambda}$ in comparison with different experimental results [38].

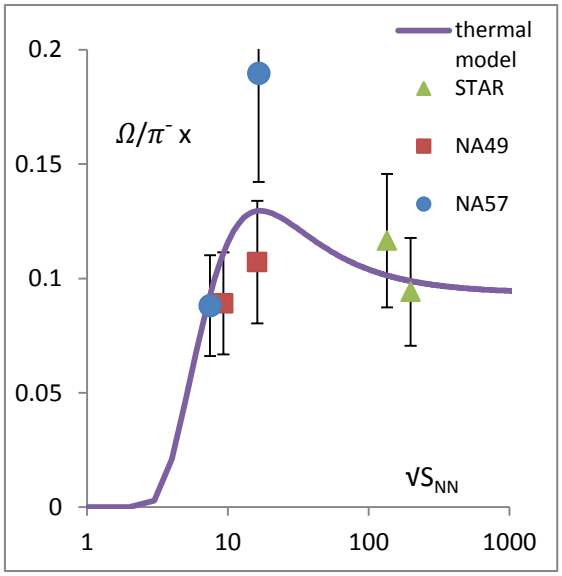

Fig 3f. The energy dependence of particle ratios for $\frac{\Omega}{\pi^-}$ in comparison with different experimental results [38].

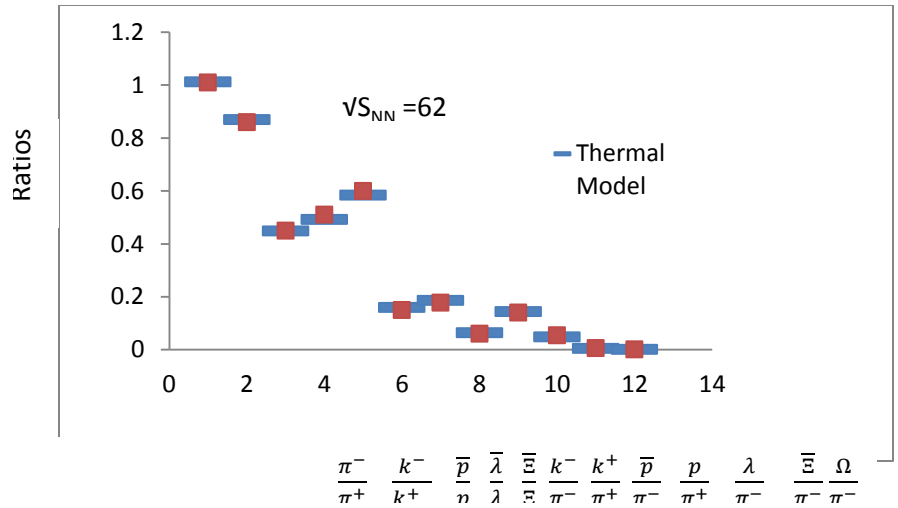

Fig 3g. Calculated Particle ratios at $\sqrt{S_{NN}}$=62 GeV in comparison with STAR experiment

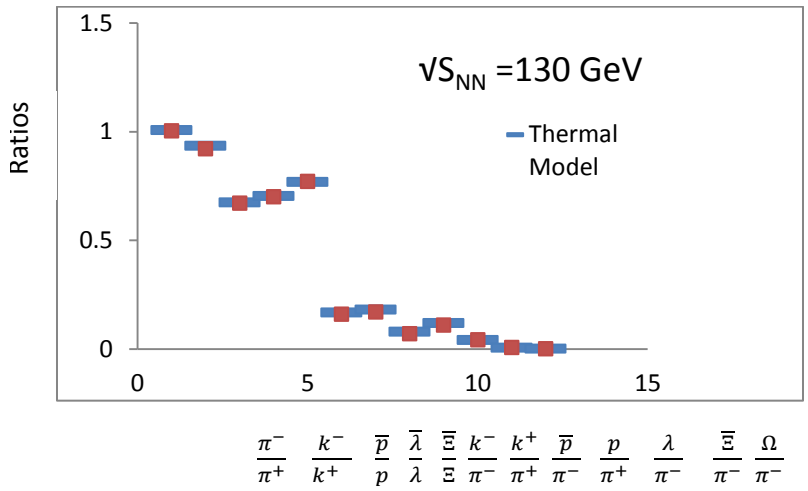

Fig 3h. Calculated Particle ratios at $\sqrt{S_{NN}}$=130 GeV in comparison with STAR experiment [29].

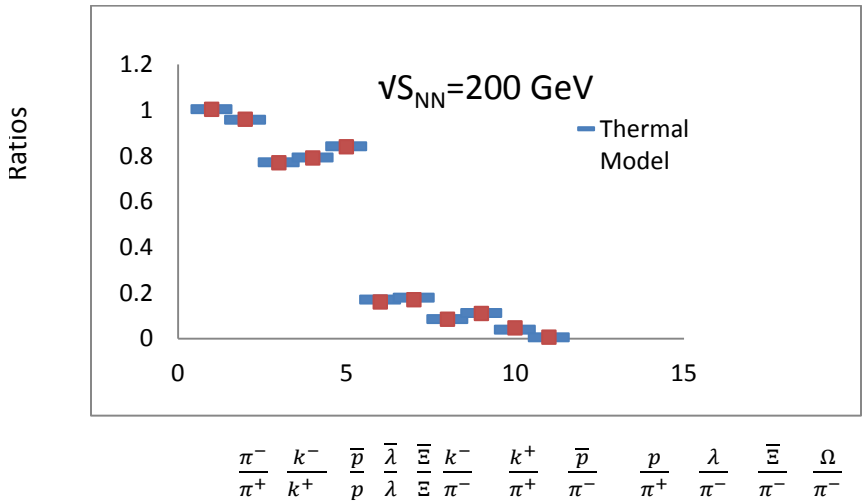

Fig 3i. Calculated Particle ratios at $\sqrt{S_{NN}}$=200 GeV in comparison with STAR experiment

5- Conclusion

In this paper, the four different freeze-out conditios which mentioned above have been calculated and compared with the avaliable experimental data. One can see that, the freeze-out temperature is approximately of $164 \leq T_f \leq 169$ MeV, which is close to the one expected for phase transition, which is about 170 MeV [51]as indicated by lattice gauge theory.

Also, The net charge fluctuations as a signal of quark-gloun plasma (QGP) are calculated in terms of the parameter ν_{dyn} . We calculated the charge dependence of the dynamical K/π, P/π, and K/P fluctuations. Only the $\nu_{dyn,k/\pi}$ in case of $\frac{K}{\pi} = \frac{K^+ + K^-}{\pi^+ + \pi^-}$ have positive values.

The energy dependence of the particle ratios $\frac{\pi^-}{\pi^+}$, $\frac{K^-}{K^+}$, $\frac{K^-}{\pi^-}$, $\frac{P^-}{P}$, $\frac{\Lambda^-}{\Lambda}$, and 10 x $\frac{\Omega}{\pi^-}$ are calculated in comparison to the avaliable results from different experiments. The particle ratios $\frac{\pi^-}{\pi^+}$, $\frac{k^-}{k^+}$, $\frac{\overline{p}}{p}$, $\frac{\overline{\lambda}}{\lambda}$, $\frac{\overline{\Xi}}{\Xi}$, $\frac{k^-}{\pi^-}$, $\frac{k^+}{\pi^+}$, $\frac{\overline{p}}{\pi^-}$, $\frac{p}{\pi^+}$, $\frac{\lambda}{\pi^-}$, $\frac{\overline{\Xi}}{\pi^-}$, and $\frac{\Omega}{\pi^-}$ are calculated at STAR beam energies 62, 130, and 200 GeV.

References

[1] A.Tawfik, Phys.Rev.D71, 054502 (2005).

[2] A.Tawfik, J.Phys.G, G31, S1105-S1110 (2005).

[3] K.Rajagopal and F.Wilczek, hep-ph/0011333.

[4] F. Karsch, K. Redlich, A. Tawfik, Eur. Phys. J. C 29, 549 (2003).

[5] F. Karsch, K. Redlich, A. Tawfik, Phys. Lett. B 571, 67 (2003).

[6] K. Redlich, F. Karsch, A. Tawfik, J. Phys. G 30, S1271 (2004).

[7] A.Tawfik, Indian J. Phys. 85, 755–766 (2011).

[8] A.Tawfik, Prog. Theor. Phys. 126, 279–292 (2011).

[9] A.Tawfik, Nucl. Phys. A 859, 63–72 (2011).

[10] A.Tawfik, Int. J. Theor. Phys. 51, 1396–1407 (2012).

[11] P. Braun-Munzinger, K. Redlich, J. Stachel, in *Quark Gluon Plasma 3*, Eds. R. Hwa, X.-N.Wang, (World Scientific, Singapore, 2004) p. 491 , nucl-th/0304013.

[12] A. Andronic, P. Braun-Munzinger and J. Stachel, Nucl. Phys. A 772,167 (2006); nucl-th/0511071v3.

[13] Andronic, P. Braun-Munzinger and J. Stachel, nucl-th/0812.1186v3.

[14] G.D. Yen, M.I. Gorenstein, Phys. Rev. C 59, 2788 (1999).

[15] G. D. Yen, M. I. Gorenstein, W. Greiner and S. N. Yang, Phys. Rev. C 56, 2210 (1997).

[16] A. Andronic, P. Braun-Munzinger, J. Stachel and M. Winn, nucl-th/1201.0693v1.

[17] S. Wheaton, J. Cleymans, hep-ph/0407174.

[18] L. M. Satarov, M. N. Dmitriev and I. N. Mishustin, Phys. Atom. Nucl. 72, 1390 (2009).

[19] K. Redlich, S. Wheaton, J. Cleymans, H. Oeschler. Phys. Rev. C, 73, 054905(2006).

[20] A. Keranen, E. Suhonen, K. Redlich, F. Becattini, J. Cleymans. Phys. Rev. C, 64, 024901(2001).

[21] H. Satz, J. Cleymans, Z. Phys.c, 57, 135 (1993).

[22] K. Redlich, J. Cleymans, H. Oeschler. Phys. Rev. C, 59, 1663 (1999).

[23] M. Kaneta, S. Wheaton, N. Xu, J. Cleymans, B. Kampfer. Phys. Rev. C, 71, 054901 (2005).

[24] A.Faessler, E. Zabrodin, L. Bravina, C. Fuchs. Phys. Rev. C, 66, 014906 (2002).

[25] J. P. Wessels, N. Xu, P. Braun-Munzinger, J. Stachel. Phys. Lett. B, 344, 43 (1995).

[26] J. Stachel, P. Braun-Munzinger, I. Heppe. Phys. Lett. B, 465, 15 (1999).

[27] K. Redlich, J. Stachel, P. Braun-Munzinger, D. Magestro. Phys. Lett. B, 518, 41 (2002).

[28] Mariusz, nucl-th/0112044v1 (2005).

[29] P. Braun-Munzinger, K. Redlich, J. Stachel, nucl-th/0304013v1 3 Apr 2003.

[30] J. Stachel, P. Braun-Munzinger, I. Heppe. Phys. Lett. B, 465, 15 (1999).

[31] J. Stachel, Nucl. Phys. A, 654, 119c (1999).

[32] K. Redlich, Nucl. Phys. A, 749, 14 (2005).

[33] K. Redlich, J. Cleymans. Phys. Rev. Lett, 81, 5284 (1998).

[34] K. Redlich, J. Cleymans. Phys. Rev. C, 61, 054908 (1999).

[35] K. Redlich, S. Wheaton, J. Cleymans, H. Oeschler. Phys. Lett. B, 615, 50 (2005).

[36] P. Steinberg, S. Wheaton, J. Cleymans, M. Stankiewicz. arxiv:nucl-th, (0506027), 2005.

[37] A.Tawfik, hep-ph/1308.1712v1(2013).

[38] A.Andronic , P. Braun-Munzinger , J. Stachelar, nucl-th/0511071v3 27 Mar (2006).

[39] P. Braun-Munzinger, J. Stachel, J. P. Wessels, N. Xu, Phys. Lett. B, 344, 43(1995), nucl-th/9410026, Phys.Lett.B3, 65, 1 (1996) nucl-th/9508020.

[40] R. Averbeck, R. Holzmann, V. Metag, R. S. Simon, Phys. Rev. C 67, 024903 (2003), nucl-ex/0012007.

[41] P. Braun-Munzinger, I. Heppe, J. Stachel, Phys. Lett. B 465, 15 (1999) nucl-th/9903010.
[42] P. Braun-Munzinger, D. Magestro, K. Redlich, J. Stachel, Phys. Lett. B 518, 41 (2001), nucl-th/0105229.
[43] W. Broniowski, W. Florkowski, M. Michalec, Acta Phys. Polon. B33, 761 (2002), nucl-th/0106009; W. Broniowski, W. Florkowski, Phys. Rev. C 65, 064905 (2002), nucl-th/0112043.
[44] M. Kaneta, N. Xu, nucl-th/0405068. J. Adams et al. (STAR), Nucl. Phys. A 757, 102 (2005), nucl-ex/0501009.
[45] J. Adams et al. (STAR), Nucl. Phys. A 757, 102 (2005), nucl-ex/0501009.
[46] T. J. Tarnowsky (for the STAR Collaboration), nucl-ex/ 1201.3336v1 16 Jan 2012.
[47] B.I. Abelev (for the STAR Collaboration), nucl-ex/0901.1795v113 Jan (2009).
[48] K. Redlich, S. Wheaton, J. Cleymans, H. Oeschler. Phys. Rev. C, 73, 054905 (2006).
[49] J. Adams (for the STAR Collaboration), nucl-ex/0307007v1 8 Jul (2003).
[50] B.I. Abelev (for the STAR Collaboration), nucl-ex/0807.3269v1 21 Jul (2009).
[51]] E. Laermann, Nucl.Phys. A, 610,1c (1996).